AD-A044 324 NAVAL POSTGRADUATE SCHOOL MONTEREY CALIF F/G 20/4
FLUID IMPACT FORCES ON CYLINDERS IN HARMONIC FLOW.(U)
JUN 77 R A POST

UNCLASSIFIED NL

ADA044324

END
DATE FILMED
10-77
DDC

# NAVAL POSTGRADUATE SCHOOL
## Monterey, California


# THESIS

FLUID IMPACT FORCES ON CYLINDERS

IN HARMONIC FLOW

by

Richard A. Post

June 1977

Thesis Advisor: T. Sarpkaya



**Approved for public release; distribution unlimited.**

SECURITY CLASSIFICATION OF THIS PAGE (When Data Entered)

# REPORT DOCUMENTATION PAGE

READ INSTRUCTIONS BEFORE COMPLETING FORM

1. REPORT NUMBER

2. GOVT ACCESSION NO.

3. RECIPIENT'S CATALOG NUMBER

4. TITLE (and Subtitle) (6)
Fluid Impact Forces on Cylinders in Harmonic Flow.

(9)
5. TYPE OF REPORT & PERIOD COVERED
Master's Thesis; June 1977

6. PERFORMING ORG. REPORT NUMBER

7. AUTHOR(s) (10)
Richard A. Post

8. CONTRACT OR GRANT NUMBER(s)

9. PERFORMING ORGANIZATION NAME AND ADDRESS
Naval Postgraduate School
Monterey, California 93940

10. PROGRAM ELEMENT, PROJECT, TASK AREA & WORK UNIT NUMBERS

11. CONTROLLING OFFICE NAME AND ADDRESS (11)
Naval Postgraduate School
Monterey, California 93940

12. REPORT DATE
June 1977

13. NUMBER OF PAGES
47

14. MONITORING AGENCY NAME & ADDRESS (if different from Controlling Office)
Naval Postgraduate School
Monterey, California 93940 (12) 47 p.

15. SECURITY CLASS. (of this report)
Unclassified

15a. DECLASSIFICATION/DOWNGRADING SCHEDULE

16. DISTRIBUTION STATEMENT (of this Report)

Approved for public release; distribution unlimited.

17. DISTRIBUTION STATEMENT (of the abstract entered in Block 20, if different from Report)

18. SUPPLEMENTARY NOTES

19. KEY WORDS (Continue on reverse side if necessary and identify by block number)

Wave impact forces; wave slamming forces; slamming coefficients; force coefficients; circular cylinders.

20. ABSTRACT (Continue on reverse side if necessary and identify by block number)

The evolution of forces acting on horizontal cylinders subjected to impact by an harmonically oscillating free surface has been investigated both theoretically and experimentally.

The experiments were carried out in a large U-shaped water tunnel, with cylinder diameters ranging from 3.0 to 6.5 inches. The results have been expressed in terms of two force coefficients. The first is — next page

DD FORM 1 JAN 73 1473 EDITION OF 1 NOV 65 IS OBSOLETE
S/N 0102-014-6601 | 1 SECURITY CLASSIFICATION OF THIS PAGE (When Data Entered)
(Page 1)

251 450

the slamming coefficient which expresses the normalized force acting on the cylinder at the time of impact; and the second is the maximum drag coefficient which occurs when the cylinder is immersed approximately 1.75 diameters in water. The slamming coefficient was found to be equal to $\pi$, as predicted theoretically. It was also found that the slamming coefficient may be amplified to a value as high as $2\pi$ through the dynamic response of the cylinder. The maximum of the normalized force in the drag dominated region was found to be approximately equal to 2.0. It decreased with increasing Froude numbers to a value of about unity.

It is recommended that further experiments be conducted with sand-roughened cylinders and the dependence of the rate of rise of the impact force on the flow parameters be investigated.

Approved for public release; distribution unlimited

# Fluid Impact Forces on Cylinders in Harmonic Flow

by

Richard A. Post
Lieutenant, United States Navy
B.S.,E.E., University of Michigan, 1969

Submitted in partial fulfillment of the
requirements for the degree of

MASTER OF SCIENCE IN MECHANICAL ENGINEERING

and the degree of

MECHANICAL ENGINEER

from the

NAVAL POSTGRADUATE SCHOOL
June 1977

Author Richard A. Post

Approved by: Thesis Advisor

Chairman, Department of Mechanical Engineering

Dean of Science and Engineering

## ABSTRACT

The evolution of forces acting on horizontal cylinders subjected to impact by an harmonically oscillating free surface has been investigated both theoretically and experimentally.

The experiments were carried out in a large U-shaped water tunnel, with cylinder diameters ranging from 3.0 to 6.5 inches. The results have been expressed in terms of two force coefficients. The first is the slamming coefficient which expresses the normalized force acting on the cylinder at the time of impact; and the second is the maximum drag coefficient which occurs when the cylinder is immersed approximately 1.75 diameters in water. The slamming coefficient was found to be equal to $\pi$, as predicted theoretically. It was also found that the slamming coefficient may be amplified to a value as high as $2\pi$ through the dynamic response of the cylinder. The maximum of the normalized force in the drag dominated region was found to be approximately equal to 2.0. It decreased with increasing Froude numbers to a value of about unity.

It is recommended that further experiments be conducted with sand-roughened cylinders and the dependence of the rate of rise of the impact force on the flow parameters be investigated.

TABLE OF CONTENTS

LIST OF FIGURES

## NOMENCLATURE

| | |
|---|---|
| $A$ | Amplitude of the wave motion |
| $A_i$ | Immersed cylinder area |
| $\bar{A}_i$ | Normalized immersed cylinder area |
| $C_h$ | Buoyancy corrected drag coefficient |
| $C_s$ | Slamming coefficient |
| $C_s^o$ | Initial value of the slamming coefficient |
| $D$ | Cylinder diameter |
| $F$ | Instantaneous total force |
| $Fr$ | Froude number |
| $f_n$ | Natural frequency (Hz), $\omega_n = 2\pi f_n$ |
| $g$ | Gravitational acceleration |
| $K$ | Keulegan-Carpenter number |
| $L$ | Length of cylinder |
| $M$ | Mass |
| $m$ | Added mass |
| $\bar{m}$ | Normalized added mass |
| $p$ | Pressure |
| $Re$ | Reynolds number |
| $r$ | Radius of cylinder |
| $s$ | Distance between pressure taps |
| $T$ | Wave period |
| $t$ | Time |
| $t_r$ | Rise time |

| | |
|---|---|
| $U_m$ | Maximum free surface velocity |
| $v$ | Instantaneous velocity |
| $v_o$ | Initial velocity |
| $z$ | Depth of cylinder immersion |
| $\bar{z}$ | Normalized depth of cylinder immersion |
| $\zeta$ | Damping coefficient |
| $\eta$ | Instantaneous height of wave surface above mean water level |
| $\eta_o$ | Height of cylinder with respect to mean water level |
| $\rho$ | Fluid density |
| $\phi$ | Velocity potential |
| $\omega_n$ | Natural frequency (rad/sec) |
| $\nu$ | Viscosity |

ACKNOWLEDGEMENTS

The author wishes to thank Professor T. Sarpkaya for suggesting the research topic and for his continual support and encouragement. In particular, the many hours devoted to this project in the laboratory are deeply appreciated. The success of this study was due, to a large degree, to Dr. Sarpkaya's innate experimental ability.

The author also wishes to thank his wife, Sandy, both for her patience and her assistance in reducing the experimental data.

# I. INTRODUCTION

Information concerning the forces acting on bluff bodies subjected to wave slamming is of significant importance in Mechanical Engineering, Ocean Engineering, and Naval Architecture. The design of structures which must survive in a wave environment is dependent on a knowledge of the forces which occur at impact, as well as on the dynamic response of the system. Two typical examples include the structural members of off-shore drilling platforms at the splash zone and the often-encountered slamming motion of ships.

The general problem of hydrodynamic impact has been studied extensively [1] motivated in part, no doubt, by its importance in ordnance and missile technology. Extensive mathematical models have been developed for cases of simple geometry such as spheres and wedges, and these models have been well supported by experiment. Unfortunately, the special case of wave impact has not been studied as extensively. Kaplan and Silbert [2] developed a solution for the forces acting on a cylinder from the instant of impact to full immersion. Dalton and Nash [3] conducted slamming experiments with a 0.5 inch diameter cylinder with small amplitude waves generated in a laboratory tank. Their data exhibited large scatter and showed no particular correlation with either the predictions of the hydrodynamic theory or identifiable wave parameters. It appears that the evaluation of the slamming effects with wavy flows is extremely difficult partly because of the limited range of wave amplitudes that can be achieved and partly because of the difficulty of measuring the fluid velocities at the instant of impact.

In essence, the present research was undertaken to extend the work of Dalton and Nash and to improve the experimental method by using a large U-shaped water tunnel. In addition, it was intended to demonstrate a correlation between theory and experiment by taking into account the dynamic response of the system. Specifically, the goals of the project were as follows:

A. to examine the existing theoretical models in determining wave slam forces on circular cylinders;

B. to furnish data, obtained under controlled laboratory conditions, about the forces acting on smooth circular cylinders subjected to impact with an harmonically oscillating water surface;

C. to determine the relative importance of the inertia dominated and drag dominated forces during wave impact; and

D. to correlate such data with respect to identifiable wave parameters such as the Froude number, Fr; the Keulegan-Carpenter number, K; and the Reynolds number, Re.

## II. THEORETICAL ANALYSIS

The traditional approach used in the design of off-shore structures involves the classical Morison equation to determine the forces due to wave motion. However, wave impact is generally defined as the early stages of the penetration of a solid body into a wave surface. At the instant of contact the fluid in the vicinity of the body undergoes large accelerations which give rise to large forces. As the body becomes more fully immersed, forces due to viscous drag and separation effects become predominant. Thus the inertia and drag coefficients used in the Morison equation are not constant, and the problem becomes very difficult, even for simple geometries.

The general case of hydrodynamic impact is usually described by using incompressible potential flow theory. For the case of a moving body with mass, M, and velocity, $v_o$, impacting a quiescent surface, the system momentum is $Mv_o$. Neglecting non-conservative forces, the momentum of the system is unchanged during penetration. However, the mass of the system increases due to the fluid which is set in motion in the vicinity of the body. Also known as "added mass", m, it results in reduction of the velocity. Thus the system momentum after penetration is $(M + m)\, v = Mv_o$. The impact force at any instant is a function of m and $\partial m/\partial t$. The solution, therefore, requires knowledge of the added mass and its time derivative.

It should be noted that viscous effects, being non-conservative, will alter this somewhat. Additionally, high speed entry (as with projectiles)

may require that compressibility effects of both the fluid and the air above it be taken into account. However, for low speed entry, these effects are generally neglected, and the fluid motion is described by a velocity potential, $\phi$, which satisfies $\nabla^2 \phi = 0$. The added mass term can then be calculated. The problem remains extremely difficult, though, because the free surface tends to "pile up" around the body. This results in an unsteady flow problem with a time dependent boundary condition (the free surface). Approximate solutions have been obtained [4] for simple shapes (spheres, cones, cylinders, wedges, flat plates, etc.) by assuming a constant plane free surface and then applying a correction for the distortion.

Kaplan and Silbert [2] developed the following relation for the force acting on a horizontal circular cylinder by a wave system which propagates normal to it, (See Fig. 1.):

$$\frac{F}{L} = \rho g A_i + (m + \rho A_i) \ddot{\eta} + \frac{\partial m}{\partial z} \dot{\eta}^2 \qquad (1)$$

in which F represents the force acting on the cylinder; L, the length of the cylinder; $\rho$, the fluid density; g, the gravitational acceleration; $A_i$, the immersed area; m, the added mass per unit cylinder length; $\eta$, the instantaneous height of the wave surface above the mean water level; and z, the instantaneous depth of cylinder immersion. The first and second derivatives of $\eta$ with respect to the time are denoted by $\dot{\eta}$ and $\ddot{\eta}$. The added mass is given by Taylor [5] as:

$$m = \frac{1}{2} \rho r^2 \left[\frac{2\pi^3}{3}\left(\frac{1-\cos\theta}{2\pi - \theta}\right) + \frac{\pi}{3}(1-\cos\theta) + (\sin\theta - \theta)\right] \qquad (2)$$

in which r represents the radius of the cylinder, and $\theta$ is defined as shown in Fig. 1.

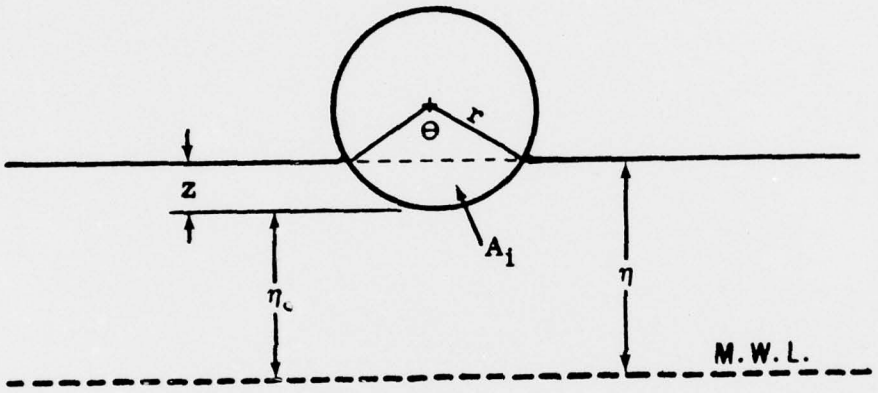


Fig. 1. Geometry for theoretical analysis of wave impact.

The motion of the free surface, $\eta$, is related to the maximum amplitude by:

$$\eta = A \sin 2\pi t/T \tag{3}$$

where A and T represent the amplitude and period of the free surface oscillations. Equation (1) can also be written in the form of a slamming coefficient, $C_s = 2F/\rho DL\, U_m^2$ as:

$$C_s = \bar{A}_i \frac{gr}{U_m^2} - (\bar{m} + \bar{A}_i) \frac{r}{A} \sin \frac{2\pi}{T} t + \frac{\partial \bar{m}}{\partial \bar{z}} \cos^2 \frac{2\pi}{T} t \tag{4}$$

where

$$\bar{A}_i = A_i/r^2 \ , \ \bar{m} = m/\rho r^2$$

$$\bar{z} = z/r \ , \ U_m = 2\pi A/T$$

With $\bar{z} = r(1-\cos \frac{\theta}{2})$, Equation (2) can be used to relate the added mass to the depth of immersion. Figure 2 is a plot of $\partial \bar{m}/\partial \bar{z}$ as a function of z/D. Clearly, $\partial \bar{m}/\partial \bar{z}$ begins with an initial value of $\pi$ and drops rapidly. The quantity $gr/U_m^2$ is related to the Froude number, Fr, by $Fr = U_m^2/2gr$. Thus $C_s = f(Fr, \frac{r}{A}, \frac{\partial \bar{m}}{\partial \bar{z}})$.

The rate of change of the normalized added mass with $\bar{z}$ depends on $\theta$ and hence on the time measured from the instant of impact (See Fig. 2). For example, for the case where $\eta_o = 0$ and $t = 0$, $\partial \bar{m}/\partial \bar{z} = \pi$ and $C_s^o = \pi$. Consequently, the for the particular case under consideration, $C_s^o$ at the instant of impact does not depend on either the size of the cylinder or the flow parameters.

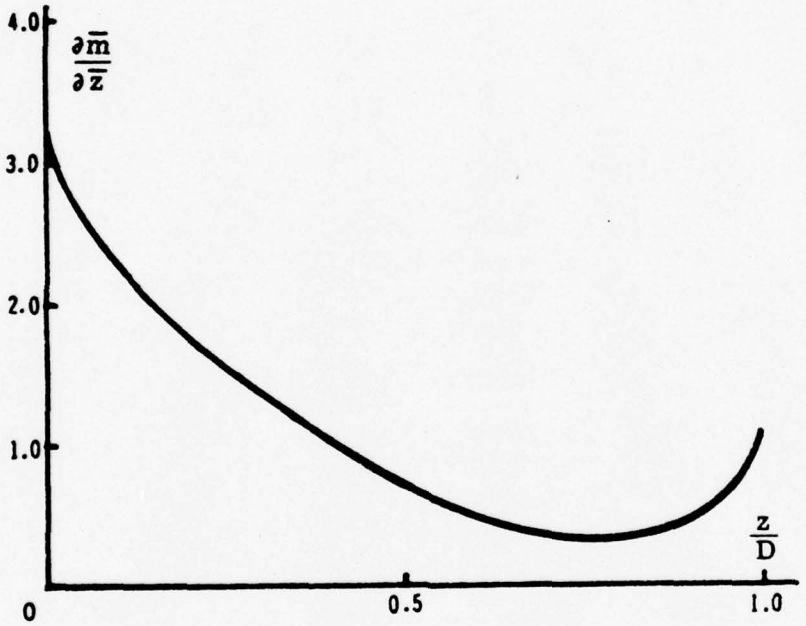


Fig. 2. $\partial \bar{m}/\partial \bar{z}$ as a function of z/D.

The fact that the cylindrical members of a structure in the splash zone are not necessarily located just at the mean water level requires the determination of the particular value of $\eta_o$ for which the slamming force at the time of impact is a maximum. It can be demonstrated through the use of Equation (4) that the maximum impact force occurs for the case of $\eta_o = 0$. For this purpose Equation (4) was evaluated with the aid of a computer program which allowed variations in r/A and $\eta_o/A$. $C_s$ was then plotted as a function of z/D from zero to unity. Figure 3 is an example of one of these plots and is typical for most cases. The variables were:

$$r/A = 0.125$$

$$\eta_o/A = 0.0,\ 0.4,\ \text{and}\ 0.8$$

As can be seen readily from Fig. 3, $C_s$ is largest at $z/D = 0$ for $\eta_o/A = 0.0$ and starts at a value of $\pi$ and drops to a minimum at z/D of approximately 0.5. It rises again as z/D approaches 1.0. Thus Equation (4) indicates that $C_s$, and consequently the impact force, is of an impulsive nature beginning with a finite value (not zero) at the instant of impact. Since viscous effects are neglected, one would expect the solution to deviate from the actual situation as the cylinder becomes more fully immersed. Where this becomes the case can only be determined by experiment.

However, one can assume that the solution would be valid for small depths of immersion, which is the case for the instant of impact up to z/D of 0.02 or so. With this restriction, $\bar{A}_i$ and $\bar{m}$ are small, as is $\sin 2\pi t/T$. Additionally, $\cos^2 2\pi t/T$ is very nearly equal to 1.0. Therefore $C_s$ reduces to:

$$C_s \approx C_s^o = (\partial \bar{m}/\partial \bar{z})_{t=0}$$

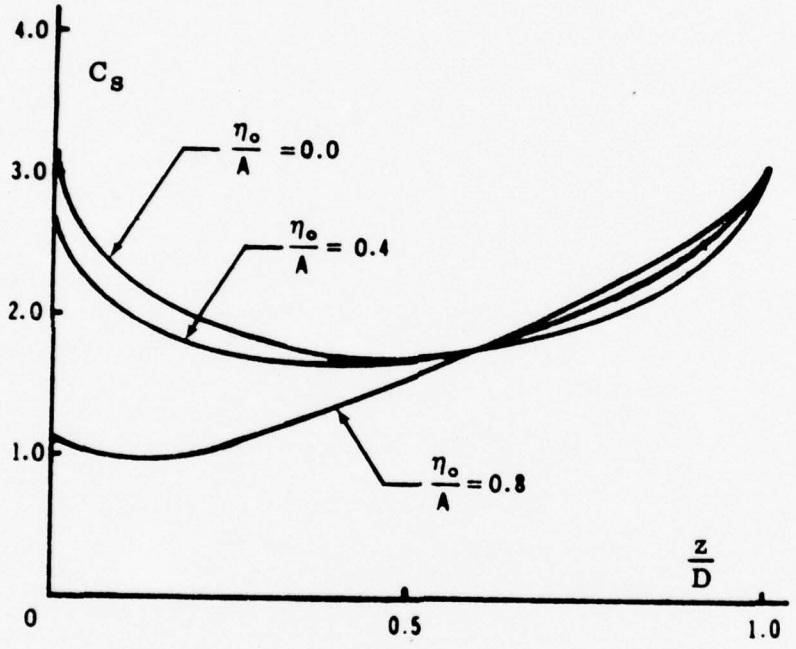


Fig. 3. Theoretical values of $C_s$ as a function of z/D for several values of $\eta_o/A$.

It is not realistic to assume that the impact force rises from zero to $\pi$ instantaneously. Several factors, specifically the compressibility of the air between the cylinder and water surface, entrapped gases in the water, and surface irregularities would account for some finite rise time. Nonetheless, the rise time can be expected to be short, i.e. in the order of milliseconds. The exact nature of the rise is an interesting question for further study. However, in this analysis $C_s$ is assumed to vary linearly during a rise period, $t_r$. For $t \geq t_r$, $C_s$ drops from $\pi$ as $\partial\bar{m}/\partial\bar{z}$. Figure 4 is a representation of this assumption. Exactly how long of a time interval $t_r$ is will be discussed later.

The realization that the impact force is of an impulsive nature requires consideration of the fact that this force does not act on a perfectly rigid body, but rather on a cylinder which is supported elastically. The response of such a system approaches that of a rigid body only if its natural frequency approaches infinity. Additionally, the response of the system to an impulsive force is heavily dependent on the exact nature of the force itself as well as on the system natural frequency.

In general, the instantaneous displacement, $x(t)$, of a system of mass, $M$, with a spring constant, $k$, is given by (See e.g. [6]):

$$x(t) = \int_0^t F(\xi)g(t-\xi)d\xi \qquad (6)$$

in which $\xi$ represents a dummy variable; $F(t)$, the driving force; and $g(t)$, the response to a unit step excitation. Equation (6) is readily recognized as the DuHamel superposition integral, which can be expanded as follows for $g(t) = \frac{1}{M\omega_n} \sin \omega_n t$:

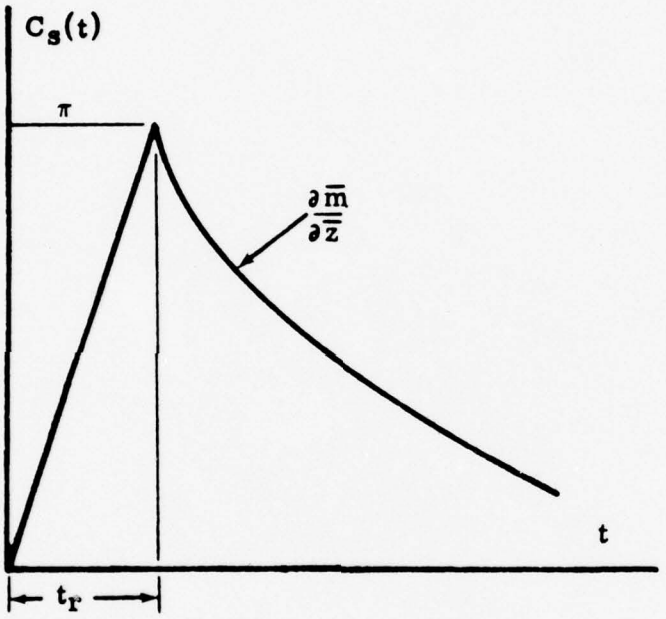


Fig. 4. $C_s(t)$ as a function of t.

$$x(t) = -\frac{1}{M\omega_n}\cos\omega_n t\int_0^t F(t)\sin\omega_n t\,dt + \frac{1}{M\omega_n}\sin\omega_n t\int_0^t F(t)\cos\omega_n t\,dt \qquad (7)$$

in which $\omega_n$ is the natural frequency of the cylinder and supports.

Letting $F(t) = F_o f(t)$ and changing the variable of integration to $\theta = \omega_n t$, one obtains

$$\frac{k\,x(t)}{F_o} = -\cos\theta\int_0^{\theta/\omega_n} f(t)\sin\theta\,d\theta + \sin\theta\int_0^{\theta/\omega_n} f(t)\cos\theta\,d\theta \qquad (8)$$

in which $k = \omega_n{}^2 M$, the spring constant. The term on the left-hand side can be interpreted as the ratio of the instantaneous force sensed by the supports of the cylinder to the actual mean force acting on the cylinder. In other words, the response of the system at time t is k x(t) which may be different from $F_o$. For the simple case in which F(t) is a step function as shown below,

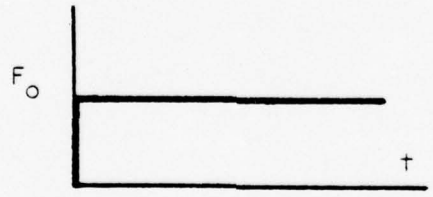


equation (8) reduces to:

$$\frac{k\,x(t)}{F_o} = (1 - \cos\omega_n t) \qquad (9)$$

It is apparent from Equation (9) that the instantaneous force sensed by the system can be anywhere from zero to two times the actual mean force.

If one assumes, as before, that the impact force is as described by Fig. 4, then Equation (8) must be evaluated using $C_s(t)$ as $F(t)$. Additionally, damping can be taken into account by writing $g(t)$ as [6]:

$$g(t) = e^{-\zeta\omega_n t} \sin \omega_n t \tag{10}$$

where $\zeta$ is the damping coefficient. Thus Equation (8) can be rewritten by replacing the forcing function, $F(t)$, by $C_s(\theta)$ as:

$$\frac{k\,x(t)}{C_s^o} = -\cos\theta \int_o^{\theta/\omega_n} C_s(\theta) e^{-\zeta\theta} \sin\theta d\theta + \cos\theta \int_o^{\theta/\omega_n} C_s(\theta) e^{-\zeta\theta} \cos\theta d\theta \tag{11}$$

Equation (11) was solved with the aid of a simple computer program which used a trapezoidal integration of variable step. Values of $\omega_n$ were taken as 358 $sec^{-1}$ and 628 $sec^{-1}$ which corresponded to the measured values of $\omega_n$ for a 6.0 inch and a 3.0 inch diameter cylinder respectively, as discussed later. The damping coefficient was 0.014 in both cases, also corresponding to measured values. The rise time was varied from zero to approximately 0.025 seconds. Figures 5 through 8 are representative plots of $\frac{k\,x(t)}{C_s^o}$ for the 6 inch cylinder, for various values of $t_r$.

Figure 5 represents Equation (11) plotted for a rise time of 0.0001 second; Fig. 6, for a rise time of 0.0100 second; Fig. 7, for a rise time of 0.0195 second; and Fig. 8, for a rise time of 0.0230 second. Note that for a very short rise time the value of $\frac{k\,x(t)}{C_s^o}$ reaches a value of approximately 1.7 at $t = 0.001$ seconds and then drops off. As the rise time increases, the value of the first peak drops off, with a "double peak" appearing at a rise time of 0.0195 seconds.

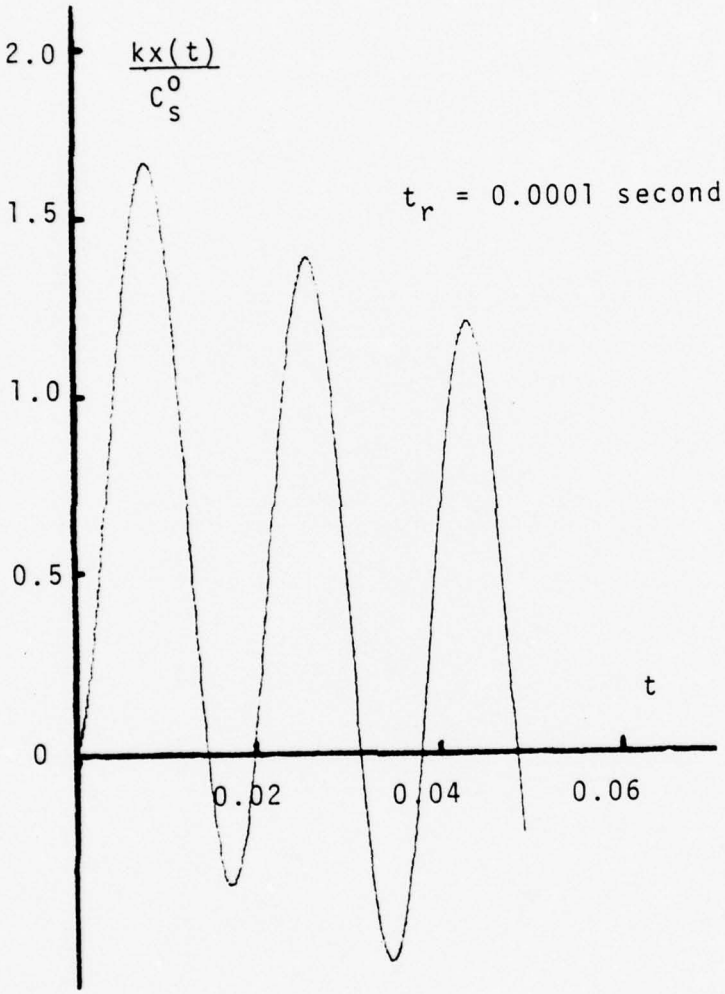


Fig. 5. $kx(t)/C_s^o$ as a function of t for $t_r$ = 0.0001 second

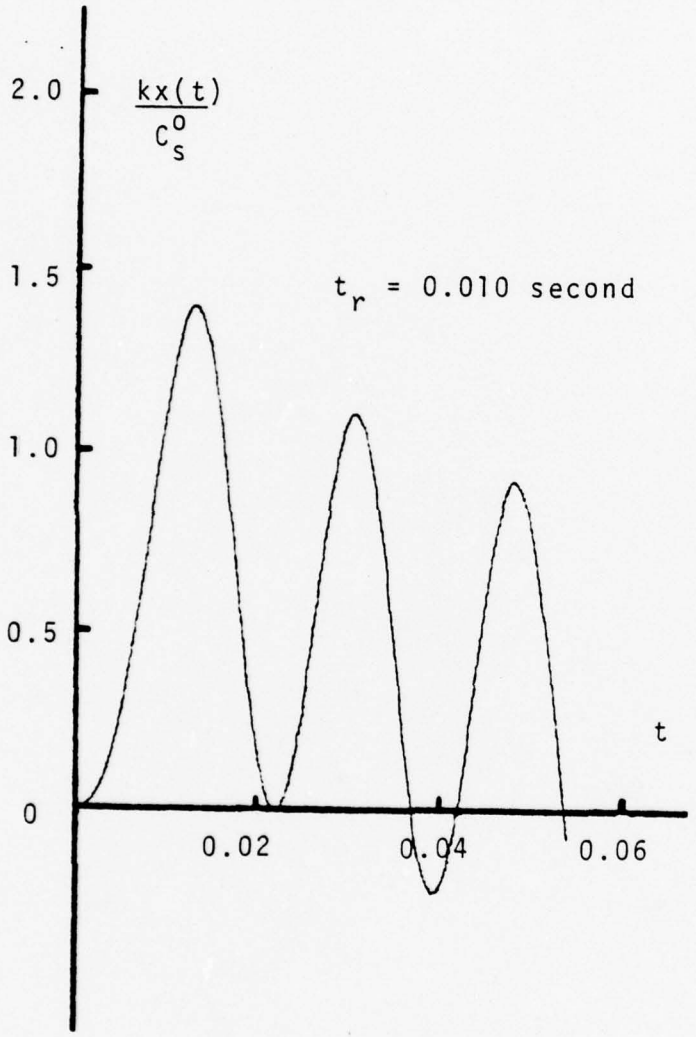


Fig. 6. $kx(t)/C_s^o$ as a function of t for $t_r$ = 0.010 second.

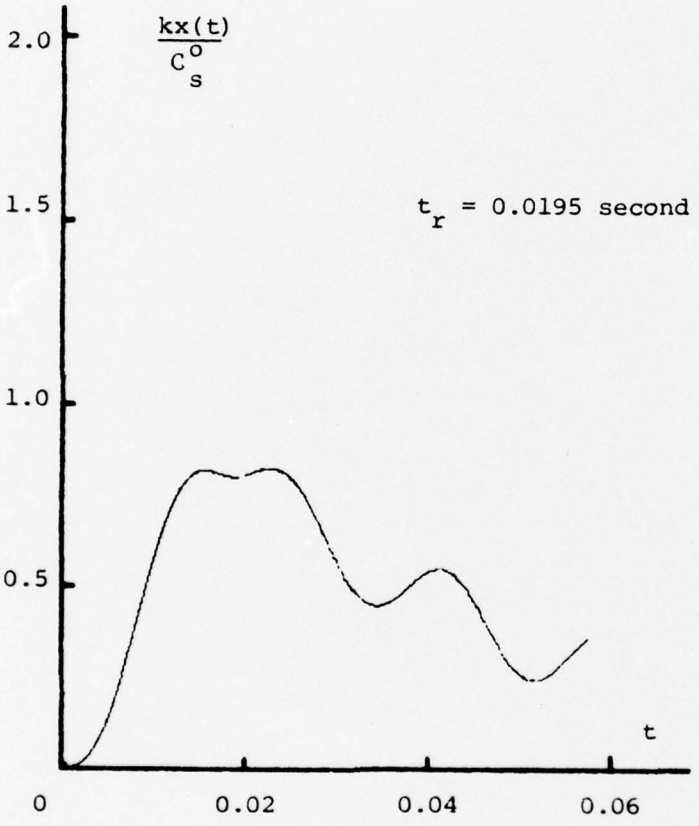


Fig. 7. $kx(t)/C_s^o$ as a function of t for $t_r = 0.0195$ second.

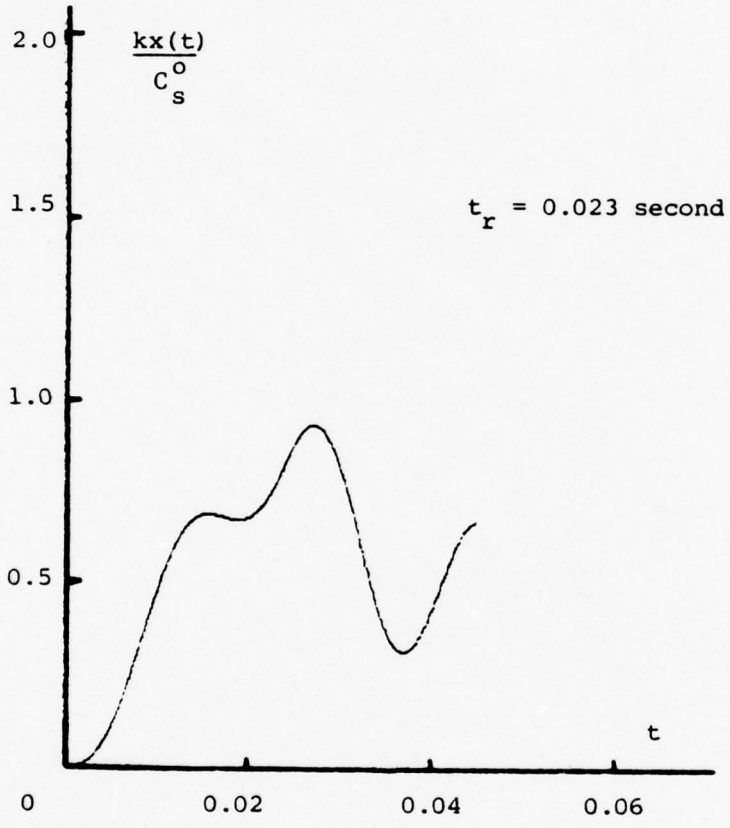


Fig. 8. $kx(t)/C_s^o$ as a function of t for $t_r = 0.023$ second.

The interpretation of the above results indicates that, depending on the rise time of $C_s(t)$, values of the apparent slamming coefficient, $C_s^o$, may lie between roughly 0.5 and 1.5 of the theoretical instantaneous value of $\pi$. Again this applies only to a small depth of immersion, corresponding to the initial moments of impact. The significance of this fact is that values of $C_s^o$ measured in the laboratory may show wide scatter depending on the rise time for any given experiment. Additionally, if the surface is not perfectly plane, rise times may vary from experiment to experiment resulting in an apparent non-repeatability.

Figure 9 is a plot of $k\, x(t)/C_s^o$ as a function of $f_n\, t_r$ for both the first and the second peak, using $\omega_n$ values for both a 6.0 inch and a 3.0 inch cylinder. From this figure, the drop in $k\, x(t)/C_s^o$ for the first peak with increasing rise time is apparent. It is also evident that the effect of $\omega_n$ is confined to a narrow range of $f_n\, t_r$ values smaller than about 0.5. The force acting on the cylinder is amplified by the dynamic response of the system for a value of $f_n\, t_r$ smaller than 0.9 and attenuated for $f_n\, t_r$ values larger than 0.9. The second peak occurs only for $f_n\, t_r$ values larger than 1.09. The value of $k\, x(t)/C_s^o$ increases from 0.84 to about unity as $f_n\, t_r$ increases from 1.09 to 1.5.

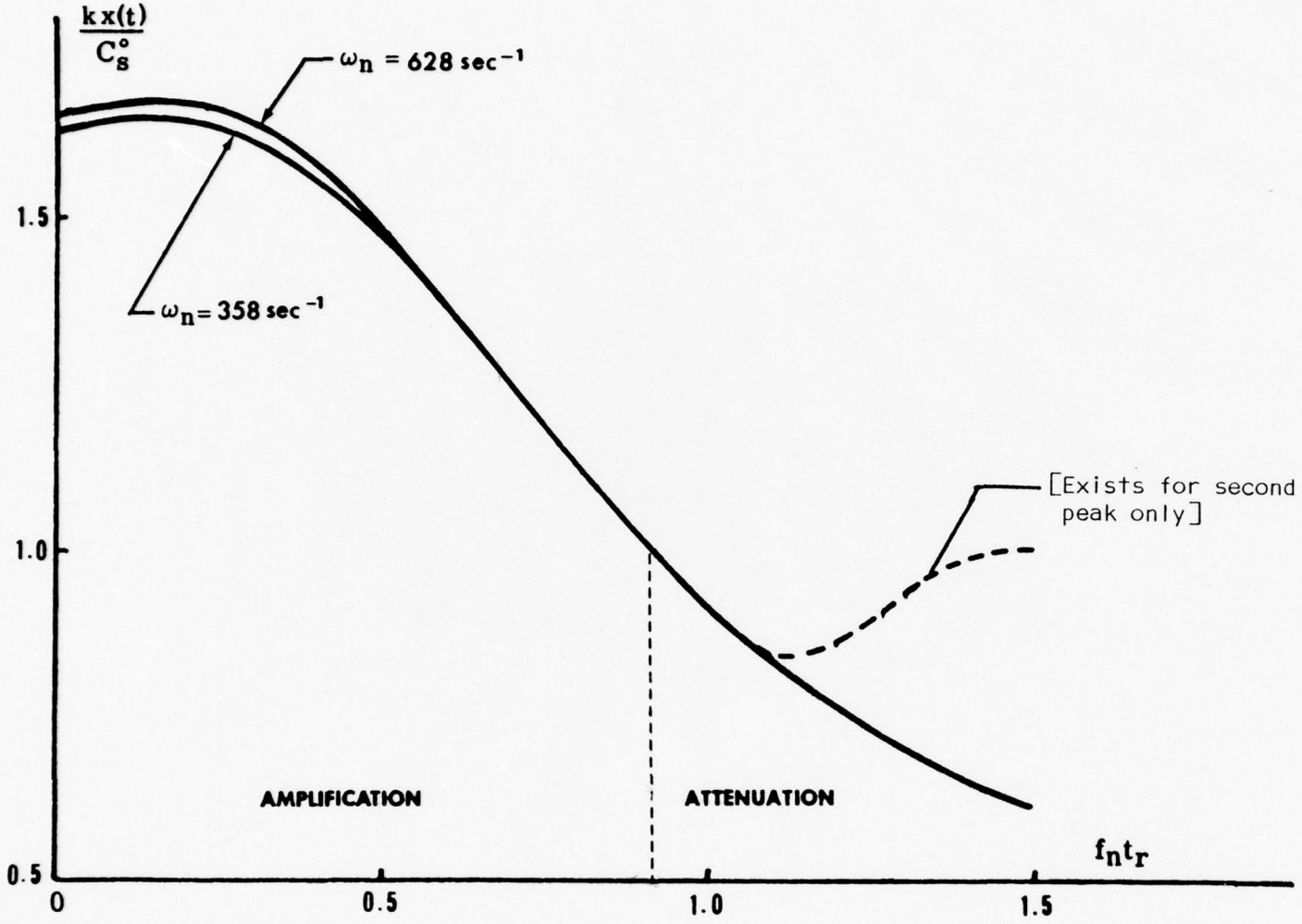


Fig. 9. $k\,x(t)/C_s^o$ as a function of $f_n t_r$.

## III. EXPERIMENTAL EQUIPMENT AND PROCEDURES

The equipment used to generate the harmonically oscillating flow has been used extensively at this facility over the past two years. The apparatus is described in reference [7]. The salient features, as well as the adaptation for this work, are briefly described in the following.

### A. U TUNNEL

Figure 10 is a schematic diagram of the U tunnel. A butterfly valve arrangement at the top of the left leg allows that side to be completely sealed off. Compressed air can then be admitted until the water level is driven to the desired height in the opposite leg. Rapid opening of the butterfly valve allows the water to oscillate at a natural frequency determined by the geometry of the tunnel. The tunnel contains approximately 5000 gallons of water and the period, T, is 5.5 seconds. Amplitudes up to 4.0 ft can be generated.

Previous work with this tunnel has demonstrated its capability in studies involving oscillating flow. Measurements have confirmed that separation does not occur at the corners and there are no discontinuities where the individual sections are joined, which might otherwise lead to disturbances in the flow. These factors were important to this project since uniformity of the free surface was a major concern.

### B. TEST CYLINDERS

Three, five, six, and six and one half inch diameter aluminum cylinders were used in measuring impact forces. Measuring 2.98 ft in

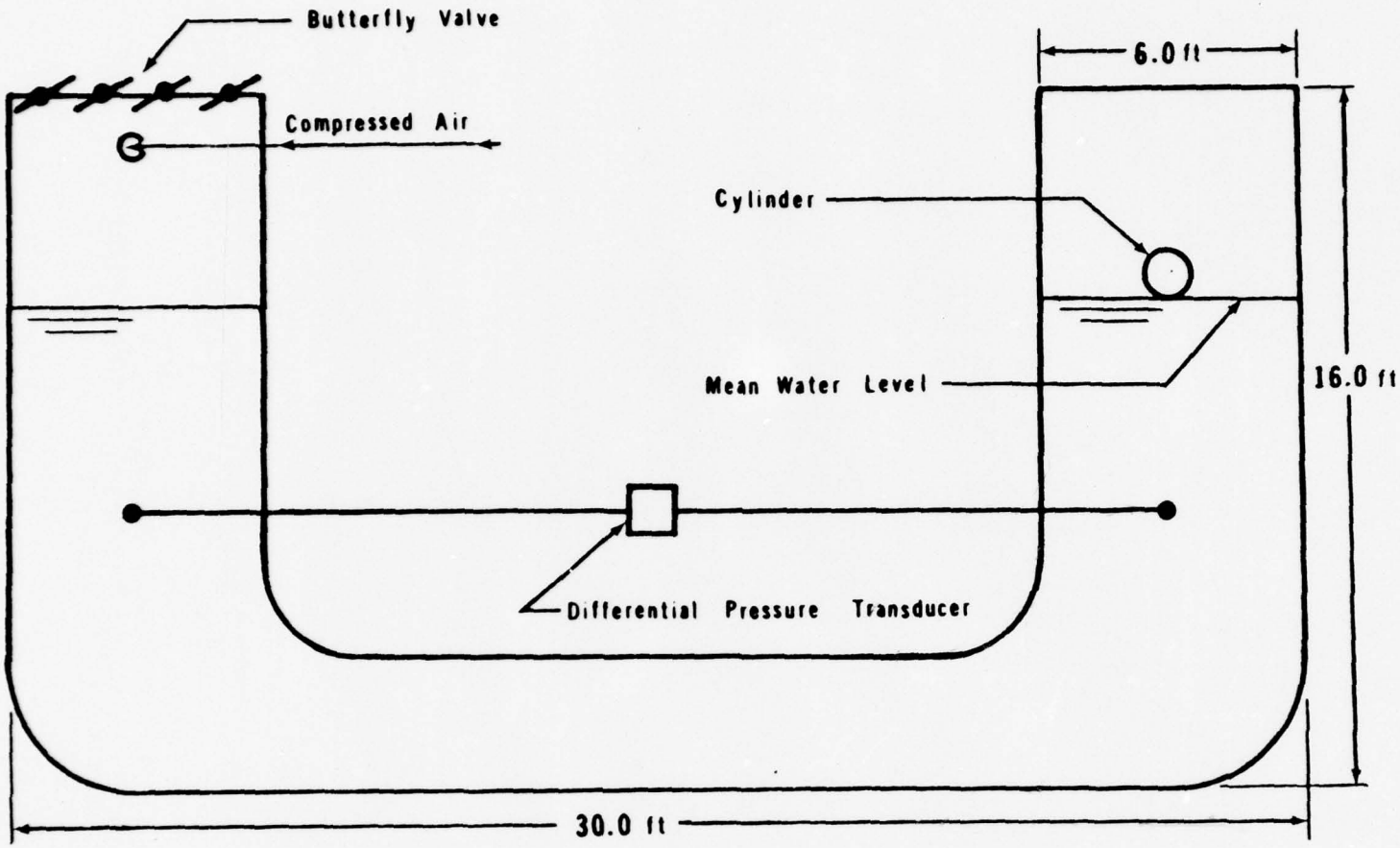


Fig. 10. Schematic diagram of the U tunnel.

length, they were constructed of aluminum pipe, turned to the final diameter, and polished to assure a hydrodynamically smooth surface. Caps fitted to each end prevented water leakage into the cylinder. Each cap contained a double precision ball-bearing mounted flush with the face. As will be noted later, the force transducers were attached to the cylinder via these bearings, and the purpose was to allow free rotation of the cylinder.

## C. FORCE MEASUREMENTS

Two cantilever-beam force transducers were used to measure the instantaneous in-line (drag) and transverse (lift) forces. The output consisted of an electrical signal from strain gages attached to the beam. The rounded end of the transducer assembly was designed to fit snugly in the bearings in the ends of the cylinders. Neoprene "O" rings were added to the end of the transducers to provide axial positioning of the cylinder within the tunnel.

Calibration of the transducers was accomplished by hanging a load from the center of the cylinder. This not only established the level of the electrical output for a known load but also reaffirmed that the transducers were correctly oriented.

As with other elements of the experimental apparatus, these transducers had been used frequently at this facility for over two years and the description of their construction may be found in reference [7]. No changes have been noted in the calibration of these transducers since their installation, a fact which establishes some degree of confidence in their use.

Initial experimental efforts established that the transverse forces were very small compared to the in-line forces, and consequently measurement of these forces was discontinued early in the study.

D. MEASUREMENT OF FLUID VELOCITY

Two pressure taps, one in each leg of the tunnel, were connected by tubing to a differential pressure transducer located midway between the taps. The acceleration of the fluid can be determined from $\Delta p = \rho s \frac{dU}{dt}$, in which $\Delta p$ represents the pressure differential; $\rho$, the fluid density; s, the distance between the taps; and $\frac{dU}{dt}$, the instantaneous acceleration of the fluid. The maximum velocity and amplitude are related to the acceleration by:

$$(\frac{dU}{dt})_m = \frac{2\pi}{T} U_m = (\frac{2\pi}{T})^2 A \qquad (12)$$

E. RECORDING EQUIPMENT

A three channel strip chart recorder was used to record simultaneously the output of the in-line force transducer and the differential pressure transducer. The third channel of the recorder was also used to record the force measurements, but the signal was first passed through a low-pass filter to remove the oscillation of the cylinder at its natural frequency, thus providing an "average" force record.

Inasmuch as the impact force to be measured consisted of a rather short rise time, the bandwidth of the recorder was of some importance. The frequency response of this recorder was flat to 100 Hz. In order to verify the response under the test conditions, several experimental runs were made in which the force was both recorded using the strip chart recorder and a tape recorder simultaneously. The taped signal was then fed back to the strip chart recorder at 1/4 speed. This method assured that the frequency response of the strip chart recorder was adequate.

F. EXPERIMENTAL PROCEDURE

The success or failure of any experimental work depends on careful attention to those factors which may have a significant effect on the measurements being taken. For this reason, extreme care was taken with all flow parameters.

Prior to filling the tunnel, the cylinder was struck lightly, and the natural frequency and damping coefficient were determined. The tunnel was then filled, immersing the cylinder several diameters, and again the natural frequency was recorded. Thus the value of $\omega_n$ was obtained both in air and in water. In the calculations the value of $\omega_n$ in air was used since at impact and shortly thereafter, the cylinder behaves as though it were not immersed.

Since the height of the mean water level with respect to the bottom of the cylinder was shown by the analysis to be important, the water level in the tunnel was adjusted carefully by slowly filling or emptying the tunnel until a slight ripple occurred at the water surface due to contact with the cylinder. This method assured that the mean water level coincided with the cylinder bottom surface.

Of paramount importance was the condition of the free surface at the instant of impact with the cylinder. Ideally the surface should be perfectly plane with no surface disturbances. It is this requirement that lends a certain degree of difficulty in the experimental procedure. Until the fluid in the tunnel has completed one cycle or so, the period of oscillation is not established. This requires that the cylinder be immersed at least once before the period of oscillation has settled down, resulting in some surface disturbance. The observations of the wave impact indicated that one slam generated minimal surface disturbances,

with the disturbances increasing with subsequent impacts. For this reason, all data were recorded for the first impact only, and successive impacts were discounted. Approximately ten minutes were allowed between each experimental run in order to allow the water surface to reach a quiescent state.

The stripchart recorder was run at a speed of 200 mm per second, each division representing 0.005 second. Figure 11 is a typical example of the data obtained. The top trace is the filtered force trace, and the bottom one is the unfiltered force trace. Figures 12 and 13 show additional unfiltered force traces for various initial flow conditions.

## G. REDUCTION OF DATA

Two force coefficients were defined in this investigation. They are:

$$C_s = \frac{2F}{\rho D L U_m^2} \tag{13}$$

and

$$C_h = \frac{2F}{\rho D L U_m^2} - \frac{g D \pi}{2 U_m^2} \tag{14}$$

The first of these refers to the slamming coefficient as defined by Equation (4). The second coefficient represents the second maximum of the normalized force with the buoyancy subtracted. This maximum occurs after the cylinder is fully immersed.

As mentioned previously, the stripchart recorder was run at 200 mm per second, thus each mm corresponded to 0.005 second. The measured force was then read each 0.005 second up to 0.5 seconds or so, depending on the diameter of the cylinder. These points were then evaluated with

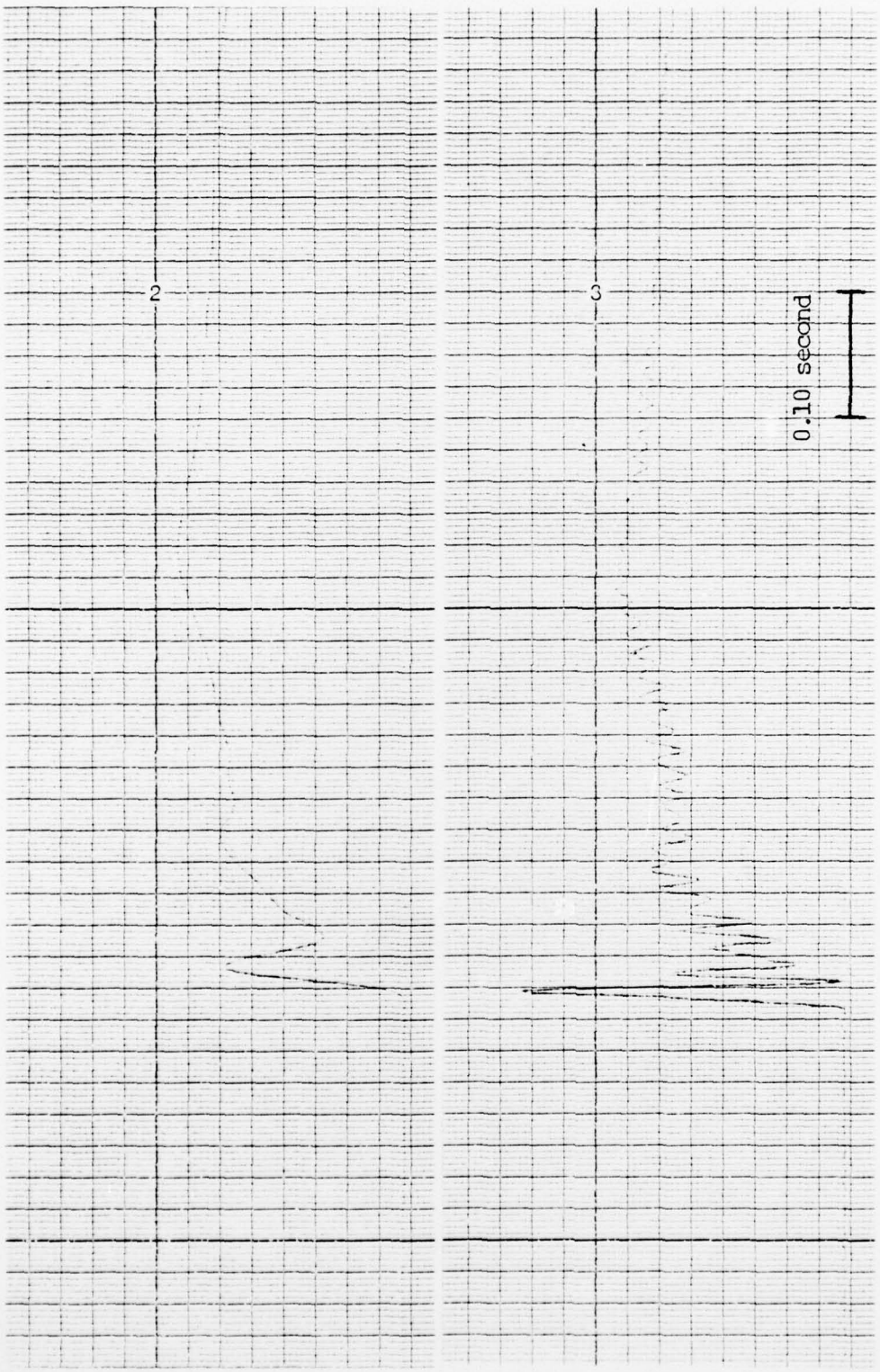


Fig. 11. Data trace showing filtered and unfiltered traces.

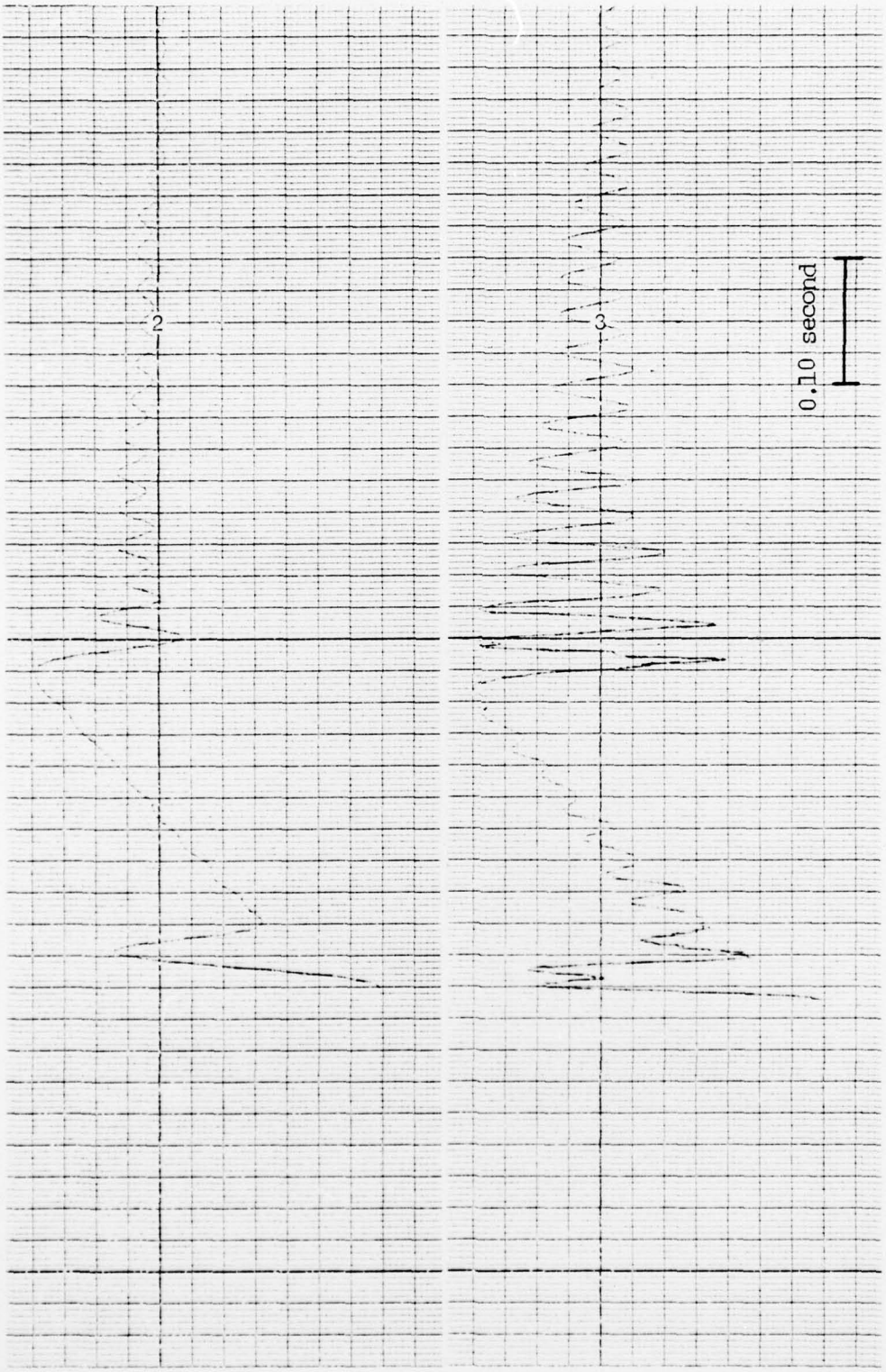


Fig. 12. Data trace for a run with double first peak.

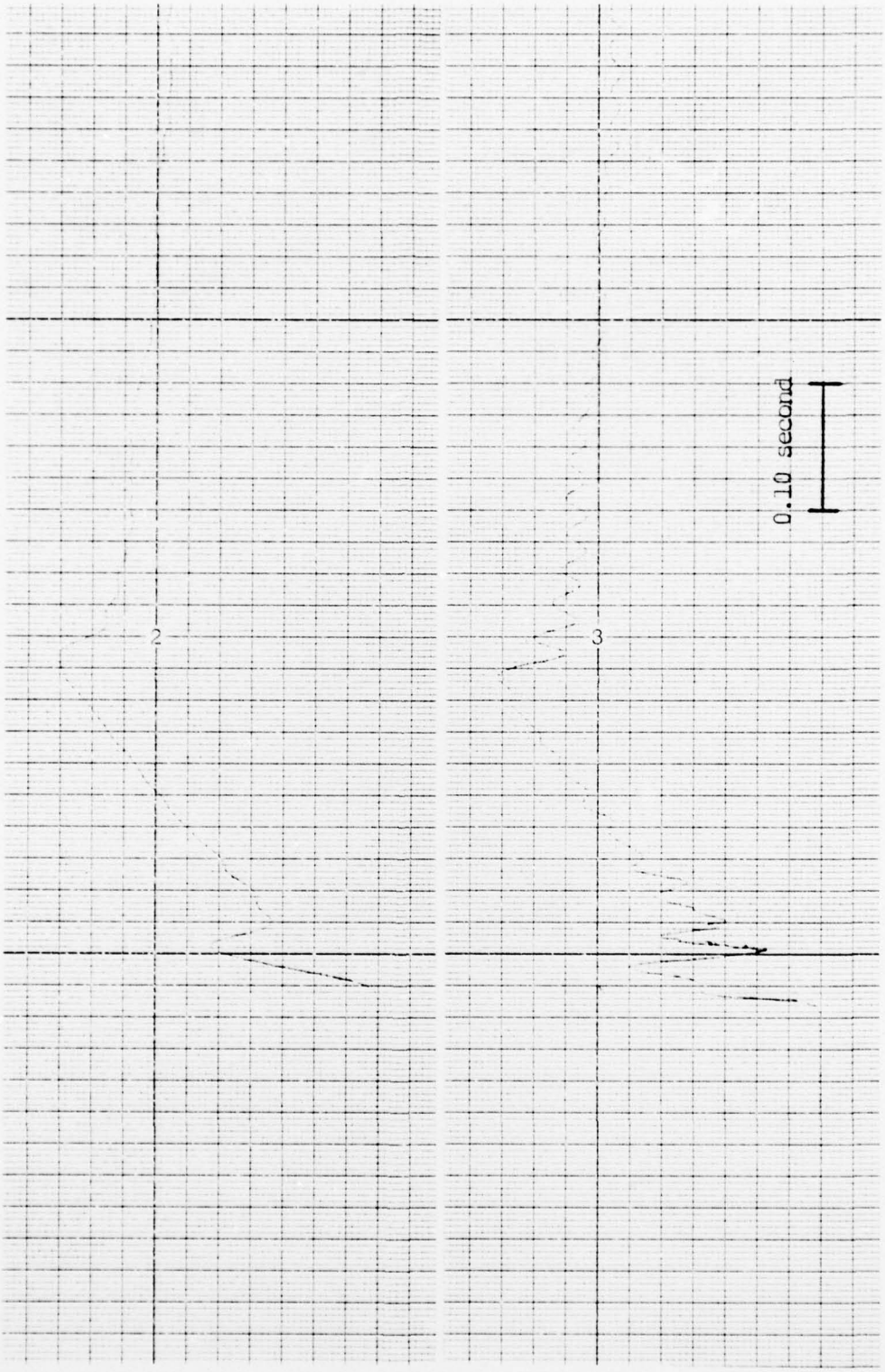


Fig. 13. Data trace for a run with decreased first peak.

the aid of a computer program which solved Equation (4) and plotted $C_s$ as a function of z/D. Figure 14 is typical of such plots, which shows the measured value of $C_s$, the theoretical value of $C_s$ from Equation (4), and the normalized buoyant force.

The filtered force trace obscured the magnitude of the initial impact. However, after the initial peak, the filtered trace was found to correspond to the average value of the unfiltered trace. Therefore, the data points during the early stage of impact were read from the unfiltered trace,and the remainder were read from the filtered trace. The main reason for this is the obvious difficulty in interpreting the average value which is obscured by the oscillation of the cylinder.

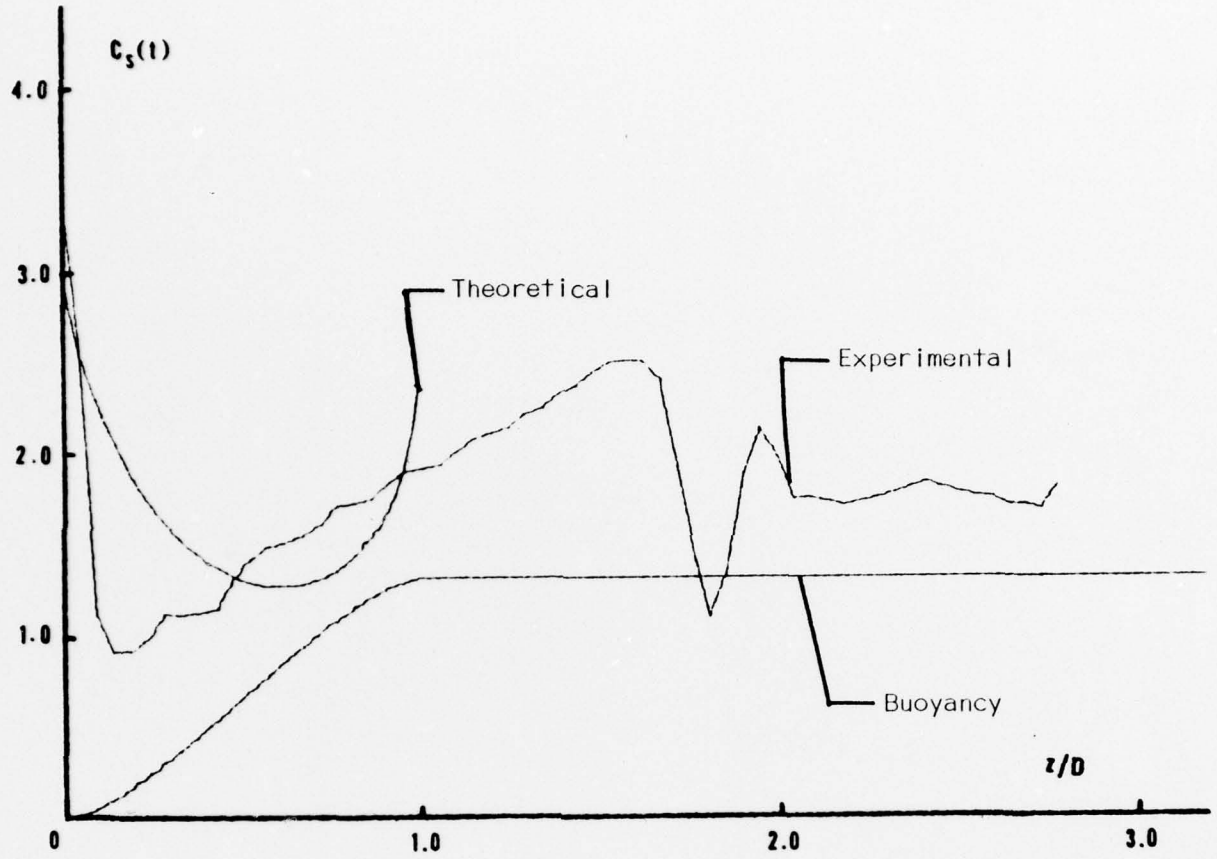


Fig. 14. $C_s$ (theoretical), $C_s$ (experimental), and buoyancy as a function of z/D.

## IV. DISCUSSION OF RESULTS

The initial value of the slamming coefficient, $C_s^o$, was plotted as a function of various parameters such as the Froude number, $Fr = \frac{U_m^2}{gD}$ ; the Reynolds number, $Re = U_m D/\nu$ ; and the Keulegan-Carpenter number, $K = U_m T/D$. These plots have revealed that there is no identifiable correlation between $C_s^o$ and the said parameters. In fact, it is the realization of this lack of correlation that led to the consideration of the rise time, $t_r$. Subsequently, the amplification or attenuation of $C_s^o$ was calculated by dividing $C_s^o$ by its theoretical value of $\pi$. Then the corresponding $f_n t_r$ values were determined from Fig. 9. Figure 15 is a plot of $f_n t_r$ as a function of the inverse Froude number $gD/U_m^2$. Even though there is considerable scatter, this figure shows that for small values of $U_m$, or large values of D, the rise time is larger and thus yields smaller amplification (See Fig. 9.). For larger impact velocities or for smaller cylinders, the rise time is considerably smaller, and the amplification factor approaches 1.7. It should be noted once more that surface irregularities, dissolved air, and other experimental uncertainties do not permit a more accurate determination of the rise time. One must add that the rise time may vary also with the physical characteristics of the fluid above the free surface, the angle of inclination of the cylinder, the length to diameter ratio, etc. Be that as it may, the Froude number appears to be the dominant parameter as in all free surface flow problems.

The physical reasoning behind the correlation of the normalized rise time, $f_n t_r$, with $gD/U_m^2$ is as follows. The disturbances in the free

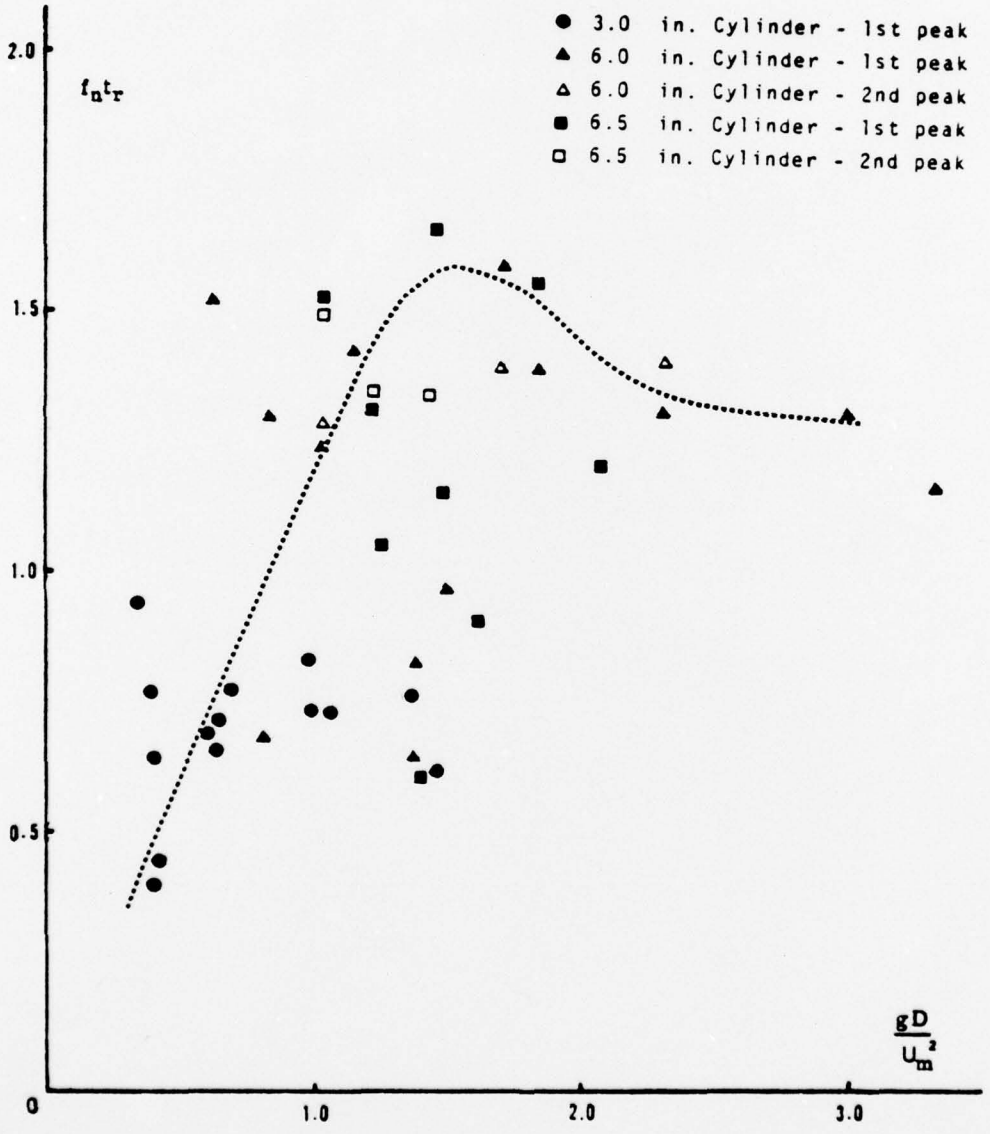


Fig. 15. $f_n\ t_r$ as a function of $gD/U_m^2 = 1/Fr$.

surface during the first passage of the flow increase with increasing diameter. On the other hand, the larger the amplitude, the longer the time for the disturbances to attenuate. Thus, the rise time decreases with increasing amplitude. Finally, the larger the acceleration of the flow, i.e. $A(2\pi/T)^2$ relative to the gravitational acceleration, the faster is the rate of attenuation of the disturbances [8,9]. A simple dimensional analysis shows, therefore, that $f_n t_r$ increases with $gD/A(T^2/A)$. Since $U_m$ is proportional to $A/T$, one finds that $f_n t_r$ is a function of $gD/U_m^2$.

A careful comparison of the measured and calculated force traces during the early stages of impact lends ample credence to the idea of rise time. Figures 5 through 8 and 11 through 13 show that for very short rise times there is a single sharp peak in the force trace. For intermediate rise times (See Figures 7 and 12.) a double peak occurs. Finally, for larger rise times (See Figures 8 and 13.) the first peak practically disappears, and the response to the slamming force is attenuated by the system.

It is event from the foregoing that the determination of the initial slamming force is extremely difficult because of its magnification or attenuation by the dynamic response of the system. The evidence presented above shows that the normalized slamming force should be assumed equal to $\pi$ and that the response of the system be determined through a straightforward vibration analysis. Such an analysis will yield the largest force amplification for a normalized rise time of $f_n t_r \simeq 0.25$. For design purposes, the maximum slamming coefficient may be as large as $1.7\pi$.

Following the initial impact, the net force acting on the cylinder begins to decrease since the $\partial\bar{m}/\partial\bar{z}$ contribution decreases. During

this stage of the flow the cylinder undergoes damped oscillations at its natural frequency. As the free surface rises further, the buoyant force increases, and the separation effects begin to give rise to larger drag forces. The buoyancy subtracted fluid force reaches its maximum at z/D values from about 1.5 to 2.0. Even though the present flow situation, in which there is a free surface, cannot be directly compared with an impulsive flow about a circular cylinder, the rise of the drag force to a maximum at $z/D \simeq 1.75$ is very much like the rise of the drag coefficient to a maximum at a relative fluid displacement of 2.0 in impulsive flow [10]. The said rise in the drag coefficient is because of the formation of two symmetrical vortices behind the cylinder. As the motion continues, the vortices become asymmetrical and shed alternatingly.

The maximum force corresponding to the second peak has been corrected for buoyancy, normalized by $\frac{1}{2} \rho U_m^2 DL$, and plotted as a function of the Froude number in Figure 16. Two facts are apparent: First, the scatter in the data is considerably less than that corresponding to the initial impact; second, $C_h$ [See Equation (14).] decreases with increasing Froude number to a value of about unity and remains nearly constant for all Froude numbers from 0.5 to 2.0.

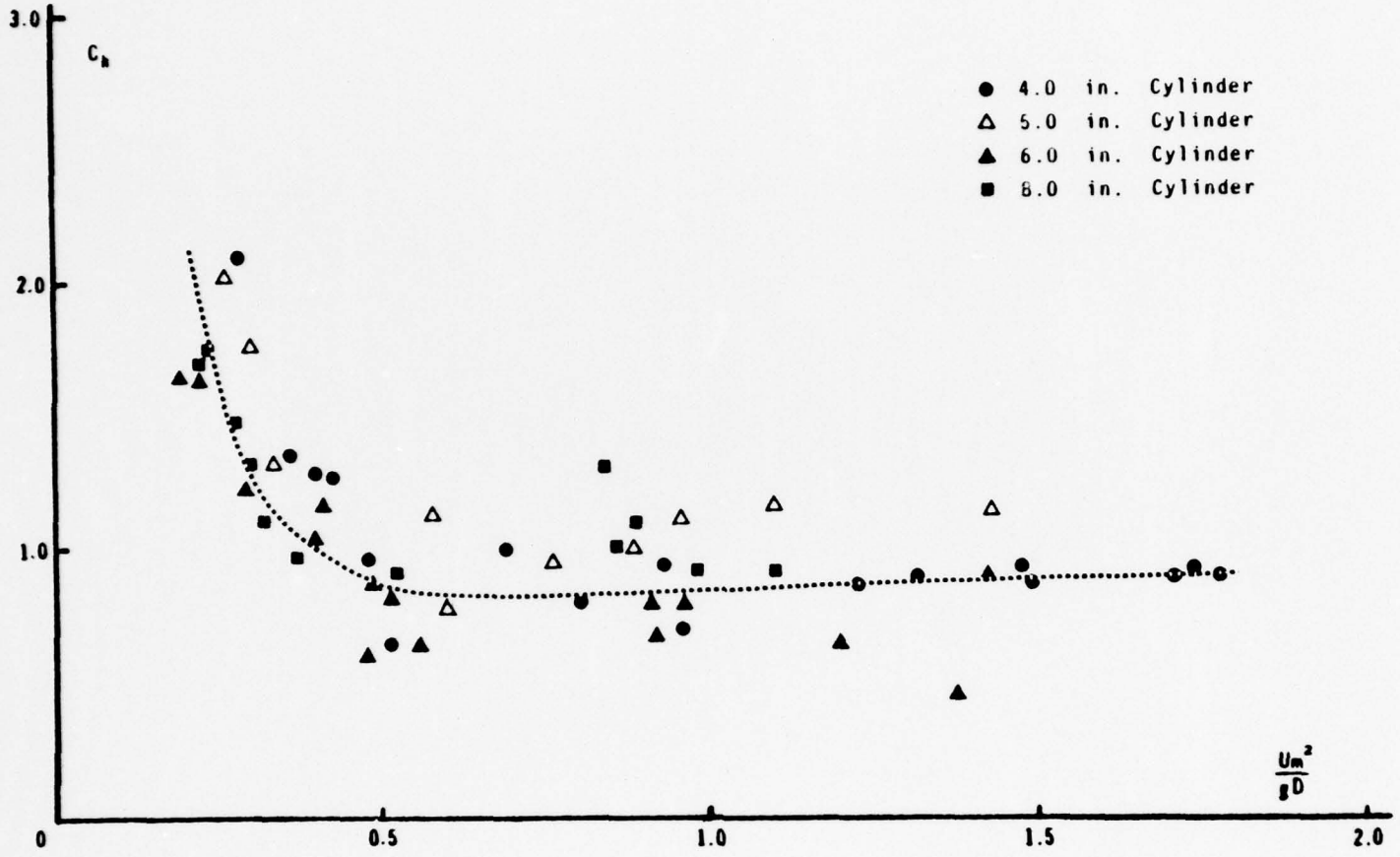


Fig. 16. $C_h$ as a function of Fr.

## V. CONCLUSIONS

The theoretical and experimental investigation of flow impact on circular cylinders warranted the following conclusions:

1. The dynamic response of the system is as important as the impact force and one cannot be determined without taking the other into consideration.
2. The initial value of the slamming coefficient is essentially equal to its theoretical value of $\pi$, and the system response may be amplified or attenuated depending upon its dynamic characteristic.
3. The normalized rise time appears to be a function of the Froude number.
4. Following the impact, the cylinder undergoes damped oscillations at its natural frequency.
5. The buoyancy corrected normalized force in the drag dominated region reaches a maximum at a relative fluid displacement of about $z/D \simeq 1.75$. Subsequently, the shedding of vortices as well as the deceleration of flow reduces the maximum drag coefficient to below unity.
6. Since it does not appear that the rise time can be determined theoretically, the dynamic response of the system should be analyzed using the theoretical value of the slamming coefficient and the experimentally determined rise times.

## LIST OF REFERENCES


1. Szebehely, V. G., "Hydrodynamic Impact", Applied Mechanics Reviews, Vol. 12, No. 5, pp. 297-300, 1959.

2. Kaplan, P. and Silbert, M. N., "Impact Forces on Platform Horizontal Members in the Splash Zone", Offshore Technology Conference, Paper No. OTC 2498, 1976.

3. Dalton, C. and Nash, J. M., "Wave Slam on Horizontal Members of an Offshore Platform", Offshore Technology Conference, Paper No. OTC 2500, 1976.

4. Chu, W. and Abramson, H. N., "Hydrodynamic Theories of Ship Slamming - Review and Extension", Journal of Ship Research, Vol. 4, pp. 9-21, 1961.

5. Taylor, J. L., "Some Hydrodynamical Inertia Coefficients", Philosophical Magazine, Series 7, Vol 9, 1930.

6. Thomson, W. T., Theory of Vibration with Applications, pp. 79-98, Prentice-Hall, Inc., 1972.

7. Collins, N. J., "Transverse Forces on Smooth and Rough Cylinders in Harmonic Flow at High Reynolds Numbers", M. S. and M. E. thesis, Naval Postgraduate School, Monterey, CA., 1976.

8. Taylor, G. I., "The Instability of Liquid Surfaces when Accelerated in a Direction Perpendicular to their Planes", Proceedings of the Royal Society of London, Ser. A, Vol. 201, pp. 192-196, 1950.

9. Benjamin, T. B. and Ursell, F., "The Stability of the Plane Free Surface of a Liquid in Vertical Periodic Motion", Proceedings of the Royal Society of London, Ser. A, Vol. 225, pp. 505-515, 1954.

10. Sarpkaya, T., "Separated Flow about Lifting Bodies and Impulsive Flow about Cylinders", Journal of the American Institute of Aeronautics and Astronautics, Vol. 4, No. 3, pp. 414-420, 1966.

INITIAL DISTRIBUTION LIST

| | | No. Copies |
|---|---|---|
| 1. | Defense Documentation Center<br>Cameron Station<br>Alexandria, Virginia 22314 | 2 |
| 2. | Library, Code 0142<br>Naval Postgraduate School<br>Monterey, California 93940 | 2 |
| 3. | Department Chairman, Code 69<br>Department of Mechanical Engineering<br>Naval Postgraduate School<br>Monterey, California 93940 | 1 |
| 4. | Professor T. Sarpkaya, Code 69SL<br>Department of Mechanical Engineering<br>Naval Postgraduate School<br>Monterey, California 93940 | 5 |
| 5. | LT. Richard A. Post<br>2498 Empire Dr.<br>West Bloomfield, Michigan 48033 | 2 |